

# Design and Implementation of Zeabus AUV for Robosub 2016

Saringkarn Pumjan, Vasutorn Siriyakorn, and Nonthanut Chuenvanich

**Abstract**—Kasetsart University has participated in Robosub since 2014. In 2016, our team has been formed by students from Kasetsart University and Chulalongkorn University to encourage collaboration between two universities. A new AUV called Zeabus has been designed in a single hull to reduce problems found in the previous years. More functions and features have been added to our software to perform more tasks, while the weight has been reduced by using lighter materials. Devices, computers, and main circuits have been installed in a single hull. Thrusters have been replaced and driver circuits have been improved in order to solve problems found in previous competitions. Zeabus AUV is operated on ROS (*Robot Operating System*).

## I. INTRODUCTION

Robosub is an international AUV competition organized by AUVERSI (Association for Unmanned Vehicle System International) foundation and is co-sponsored by ONR (Office of Naval Research). The competition is annually held at TRANSDEC facility, part of SPAWAR Systems Center Pacific in San Diego, California. The competition is designed to challenge student-built AUVs with tasks that simulate real-world missions.

The Faculty of Engineering, Kasetsart University, participated in Robosub 2014 and 2015 and was able to go into the semi-final round. Unfortunately, due to lacks of some equipment, resources, time, and experience, we could not reach the final round. In 2016, students from Kasetsart University has teamed up with students from Chulalongkorn University to redesign an AUV to improve the performance of the robot. The name of our AUV is Zeabus. This paper describes the design of Zeabus AUV and is organized as follows. Section II describes our design strategy. Section III describes mechanical design of AUV. Section IV explains electrical design including electrical structures and sensors used. Section V provides information of software implemented for AUV control and navigation. Section VI shows some experimental results. Finally, section VII ends the paper with the conclusion.

## II. DESIGN STRATEGY

Based on our experience in 2015, we have found many problems in our design as follows.

### 1) *Multiple hulls*

Originally, our team thought that separating devices and equipment into multiple hulls would enable us to perform maintenance easily. However, this plan caused more design complexity, more drag, and increased a chance to have a

leaking problem. Thus, in this year, we have decided to use a single hull to reduce design complexity.

### 2) *Materials*

Since we initially wanted our AUV to be able to run in actual sea, we used an opaque aluminum platform in the last year for more robustness. Nevertheless, when a problem happened inside a hull, the problem was difficult to be found. Using opaque aluminum also increased unnecessary weight. To avoid these problems, we have used acrylic plastic and aluminum as our main materials instead.

### 3) *Vision system*

In the previous year, our vision system did not perform well when there was bright light. We have planned to improve the performance of our vision system by using more advance algorithms.

### 4) *Hydrophone system*

Our hydrophone system could work well in the previous year during practicing in the competition. Unfortunately, an unexpected problem happened and the AUV could not surface at the right position due to a software bug in the system. We planned to debug this problem and use a more advance algorithm to reduce noises.

Other than these technical problems, we also have management problems such as limited team members, testing time, and sponsorship. To solve team member problems, a joined team from Kasetsart University and Chulalongkorn University has been formed. In order to handle our limited sponsorship problem, we have reduced some designs and equipment. However, our limited testing time due to student studying schedules is unavoidable so we have to test our AUV as much as we can do.

## III. MECHANICAL DESIGN

### A. *Zeabus Platform*

In the previous year, several electrical components were separated and installed in multiple hulls, which are difficult to access and repair. Some of sensors such as cameras and hydrophones were isolated in different hulls. This sensor installation complicated mounting positions on platform design. The multiple hull design also increased drag and unnecessary buoyancy on the vehicles. Therefore, in this year, our team decided to use a single hull design, which can contain all equipment in one hull. The new design has better accessibility and frame integrity, and also reduces drag and unnecessary buoyancy. The new Zeabus platform is shown in Figure 1.



Fig.1. Zeabus platform.

Materials used to build the Zeabus platform are aluminum, acrylic and ABS plastic. Acrylic plastic is used to build clear front and back of the main hull, while aluminum is used to build the body frame and hexagon-shape body center. This body center was built by folding an aluminum sheet into a hexagon shape, which allows us to install peripheral connectors tightly on the outer surface. On the other hand, an acrylic tube allows us to integrate the whole camera system within the single hull by using its transparent property.

The main frame structure of the Zeabus platform was made of standard profile aluminum. Thus, positions of all gadgets including torpedoes and markers can be easily adjusted. This frame also allows us to compensate COM (Center of Mass) of the vehicle by moving a bracket or some parts of the frames to nearby positions.

Battery pods are also redesigned to have less cross section area and volume in order to reduce drag and buoyancy as shown in Fig. 2.



Fig. 2. New battery pod.

**B. Gripper**

A pneumatic gripper is made of acrylic plastic and stainless steel to reduce the weight. Some gripper parts are made by 3D printing. This gripper is designed to grasp an object on both x and y axis as shown in Fig. 3.

**C. Torpedo launcher**

A Zeabus torpedo launcher shown in Fig. 4 was made of a PVC pipe. A torpedo can be launched with a power of a spring inside a launcher. A pneumatic lock is used to block a torpedo. In order to fire a torpedo, this lock is released and

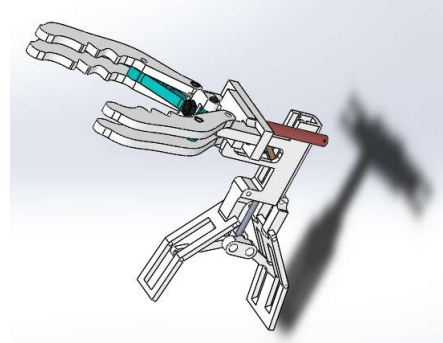


Fig. 3. Gripper.

the torpedo will be launched with a potential energy from a spring. Another torpedo launcher is used as a marker dropper. When Zeabus wants to drop a marker, the AUV just fires a torpedo downward to the target. Torpedoes were made of ABS. Since the density of ABS is close to water, a fired torpedo will not be significantly affected by buoyancy and can hit a target with more accuracy.



Fig. 4. Torpedo launcher.

**D. Pneumatic system**

A pneumatic system used to drive a gripper, fire a torpedo, and drop a marker is built by using SMC SY3100 U1 solenoid valves shown in Fig. 5, which are connected with a disposable CO<sub>2</sub> cartridge.



Fig. 5. SMC SY3100 U1 solenoid valves

**E. Thrusters**

Eight Blue Robotics T200-R1 are used as a vehicle's

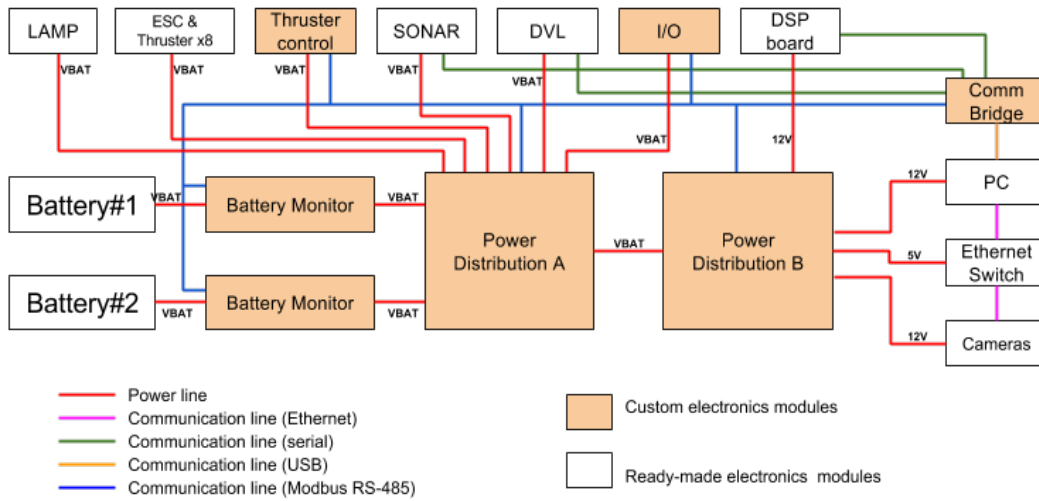


Fig. 6. Electrical module on Zeabus AUV.

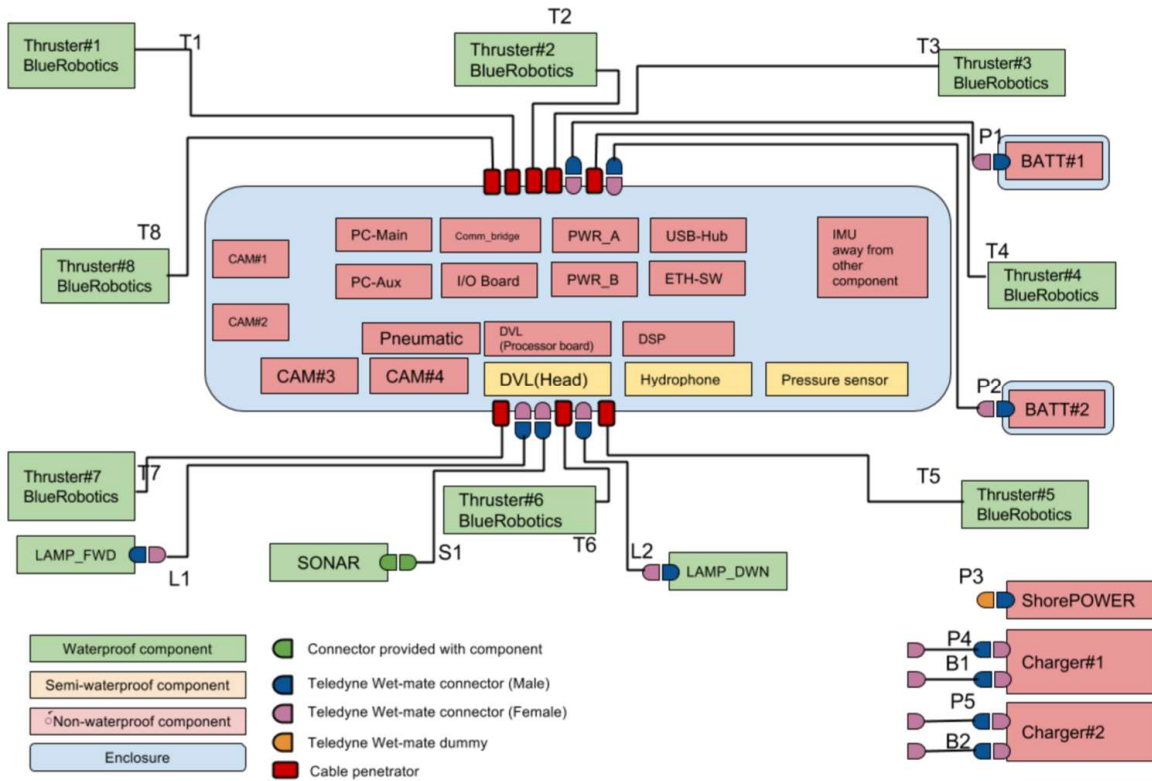


Fig. 7. External connections and diagram.

thruster on the 2016 platform because of their high thrust and light weight. Four of eight thrusters are mounted along the vertical axis to provide a high downward thrust, and the remain thrusters are mounted by 45 degree along the vehicle to provide a thrust on the xy coordinate.

#### IV. ELECTRICAL DESIGN

##### A. Electrical Architecture

Electrical parts of Zeabus AUV are divided into several modules so that they can be manufactured, tested, maintained, or upgraded separately without affecting other

subsystems. With this design concept, the system up-time can be maximized. Main design concerns of these modules are safety, ease of uses, low energy consumption, low weight, and high reliability. Also, the sizes of these modules must be fitted in limited installation areas. Electrical modules implemented on Zeabus are shown in Fig. 6 and listed as follows.

#### 1) Power distribution modules

Power distribution modules are divided into modules A and B.

##### • Power distribution module A

This module mainly transfers the power from batteries to all other modules. The module is able to protect the overall system when an overcurrent is drawn. The module will shut down the whole system if the emergency switch is activated.

##### • Power distribution module B

This power distribution module includes many isolated voltage regulators. The module draws the power from the power distribution module A to supply power to sensors, computers, and other modules that require a stable power source.

#### 2) Thruster controller module

This module controls all 8 thrusters by receiving commands from an on-board computer and generates control signals to Electronics Speed Controllers (ESC).

#### 3) Communication bridge module

This module converts signals from serial ports to USB in order to connect serial communication to an on-board computer. This module also provides signal isolation on transmitted and received signals to reduce communication noises.

#### 4) Battery monitor module

This module monitors the status of battery packs connected to the vehicle. Status monitored includes temperature, voltage, current, and charge. Monitoring this status helps operators to inspect the system and decide when the battery needs to be recharged to prevent over-discharging.

#### 5) Input-output module

This module consists of input and output ports. The input ports are used to gather the status of switches. The output ports are used to light up LEDs according to the status of the vehicle and control valves of the AUV pneumatic system.

### B. Connectors

Zeabus AUV connections use Blue Robotics cable penetrators for thruster cables and Teledyne Impulse Wet-Pluggable IL, MCIL-series connectors to connect external batteries, Ethernet network, and lamps. Teledyne connectors are specially designed for underwater environment and can be mated in wet condition. These connections are shown in Fig. 7.

### C. Computer and peripherals

There are several computers and peripherals used in the Zeabus AUV as follows

#### 1) Main PC

The main computer used to control Zeabus AUV is Intel NUC D54250WYK as shown in Fig. 8.



Fig. 8 Main computer Intel NUC D54250WYK.

#### 2) Auxiliary PC

NVIDIA Jetson TX 1 shown in Fig. 9 is used as an auxiliary PC to process computer vision tasks. This module has CUDA core to speed up computer vision tasks up to 1 TFLOPS. Vision tasks are processed together with the main PC using ROS (Robot Operating System).



Fig. 9. NVIDIA Jetson TX 1.

#### 3) Ethernet switch

An Ethernet switch used for communication in Zeabus AUV is ZyXEL GS-108B shown in Fig. 10. This switch is used because of its small size and metal housing to reduce noises and enable heat dissipation. This switch can also operate at 50 °C, while other switches usually operates at 40 °C.



Fig. 10. Zyxel GS-108B Ethernet switch

#### 4) Shorepower

This is a power supply used when the AUV is not in water. When the AUV is put on the water, the power cables supplied by Shorepower can be taken out without any interruption on

the AUV operation. The power supply used as Shorepower is MEANWELL SE-600-15.

#### 5) USB hub

A USB hub used for data transfer in AUV is Orico W6PH4.

### D. Sensors

There are several sensors used on Zeabus AUV as follows.

#### 1) Cameras

The camera model used in the AUV is IDS uEye UI-5241LE-C shown in Fig. 11. Two cameras are installed at the front of the AUV, while the other two cameras are installed at the bottom.



Fig. 11. IDS uEye UI-5241LE-C.

#### 2) DVL (Doppler Velocity Log)

A Teledyne RD Explorer DVL shown in Fig. 12 is used to measure the velocity of the AUV.



Fig. 12. Teledyne DVL.

#### 3) IMU (Inertial Measurement Unit)

The IMU used in Zeabus AUV is a Lord MicroStrain 3DM-GX4-45 shown in Fig. 13, which is mainly used as AHRSS (Altitude Head Reference System).



Fig. 13. Lord MicroStrain 3DM-GX4-45 IMU.

#### 4) Pressure sensor

A pressure sensor used on Zeabus is US331 manufactured by Measurement Specialties shown in Fig. 14. The pressure sensor is used to measure depth of the AUV.



Fig. 14. Pressure sensor.

#### 5) Hydrophone

Four TC 4013 hydrophones made by Teledyne Reson are used to sample an acoustic signal transmitted from a pinger. Four sampled signals will then be processed by a DSP (Digital Signal Processor Board). A TC 4013 hydrophones is shown in Fig. 15.



Fig. 15. Teledyne Reson TC 4013 Hydrophone.

## V. SOFTWARE DESIGN

### A. Software overview

The Zeabus software system is composed of:

#### 1) Mission planner group module

This part decides a plan, a path, and a direction of the AUV.

#### 2) Control system module

The control system module is used to control thrusters. The main control algorithm used on this module is PID control algorithm.

#### 3) Vision system module

The vision system module is used when the AUV has to navigate by using vision to finish some tasks.

### B. Mission planner group module

In mission planner group module shown in Fig. 16, there are several submodules including sensor fusion, mission planner, path planner, and trajectory generator. Sensors such as IMU, cameras, and hydrophones, will send data through communication channels, and then the sensor fusion software module will fuse all data together in order to process in the next step. This module also checks the power for operations. The mission planner module will use the fused data to choose a strategy to perform tasks based on different criteria. Once the strategy is decided, the path planner module will generate the robot path according to the

strategy. The trajectory generator will then generate actuator trajectories such that the robot will follow the generated path. These trajectories will be used as control goals for actuators such as thrusters. Other peripheral devices such as grippers, torpedo launchers, and lamps will be activated based on trajectories generated according to the strategy chosen.

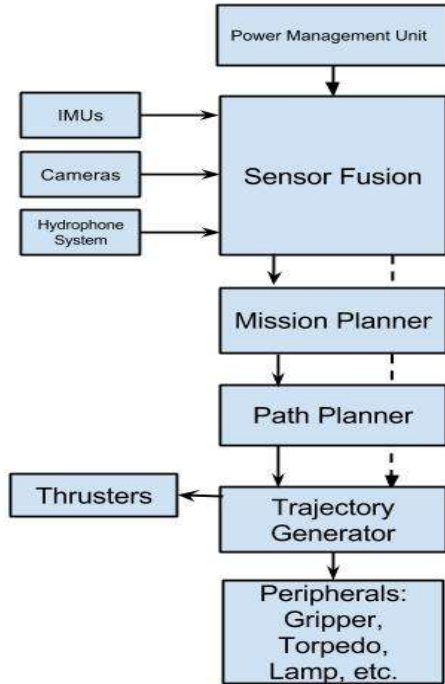


Fig. 16. Mission planner group module.

Our mission planner module is written by Python. Mission planner connects with other systems by ROS (Robot Operating System). When an AUV is performing a task, mission planner acquires and processes data from nodes. After processing, mission planner will command each node to do the task. This process is repeated until the AUV finishes a task.

C. Control system module

A PID control concept [1] shown in Fig. 17 is used to stabilize the depth and heading of our vehicle.

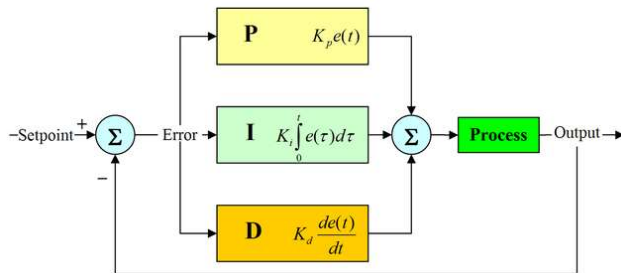


Fig. 17. Block diagram of PID control algorithm

Orientation of the robot can be estimated by fusing all measured data using Unscented Kalman Filter (UKF) [2]. Angle estimates are available as Euler angle or quaternion angle outputs. Our robot self-stabilizing algorithm uses an estimated angle and the rate of a change in angle. Eight

thrusters will be controlled in this process. Each of the outputs will be carefully calibrated to make the vehicle move in the correct path as much as possible in order to control the robot stability.

D. Vision system module

Our vision system is written by using OpenCV and TensorFlow in Python and C++, respectively. The architecture of our vision system module is shown in Fig. 18.

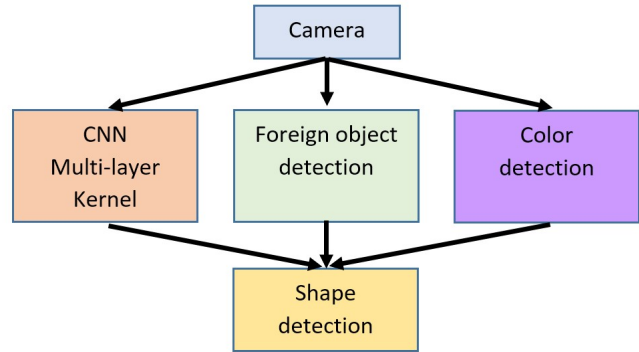


Fig. 18. Vision system architecture.

In the CNN (Convolution Neural Network) [3] module, the image kernel is generated from training data and used to detect and classify which part of the input image from the camera are informative. Then, the image will be segmented for further processing. The segmented images are then passed to Shape detection module to do further processing about the location of that object.

The foreign object detection module will initially detect if there are any objects that should not be in water, on the floor, or in the background. To perform foreign object detection, the captured image is analyzed with the hysteresis thresholding [4]. Average colors of the image are computed so that the color of the “background” can be extracted. This color is then expanded into a range in a color space, which are YUV or YCbCr as shown in Fig. 19, in order to decide what is being considered is not an object.

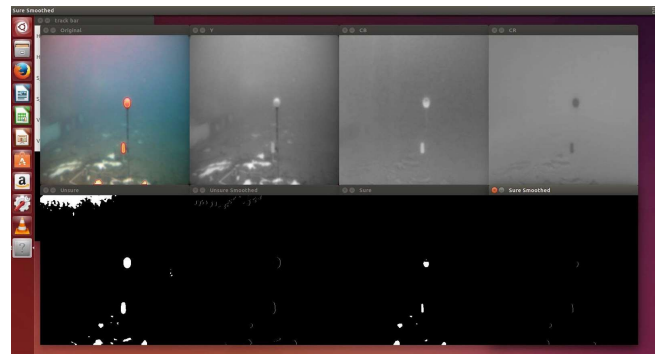


Fig. 19. Buoy in YCbCr color space.

Then, another range is created in order to confirm that the object of interests is an object. By using hysteresis thresholding, we can determine an object accurately with a strict thresholding range if it is an object of interests or not.

In the top left frame in Fig. 19, the yellow contours drawn over the image mark the part where the algorithm is sure that it is a part of an object. While the red contours mark the actual object that the algorithm recognizes. Since this method is color space independent, it can also be used with the HSV, or even the RGB color space, in case that the YCbCr color space cannot find the defining factor of the object.

The color detection module uses colors that are indexed in HSV (Hue-Saturation-Value) color space because HSV is easy to represent an index of colors by hue values. After images are acquired from AUV cameras, the imaging data are converted to HSV. The index of colors is obtained by using a user interface shown in Fig. 20 to capture an image and record a range of colors. An example of color detection to detect an underwater gate is shown in Fig. 20. This stage is needed due to a lack of object classification from Foreign object detection.

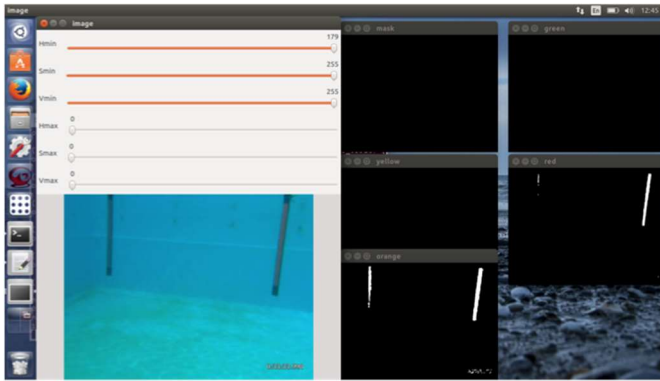


Fig. 20. Vision system interface for gate detection.

In the shape detection module, we assumed that a group of pixels has already been detected in an image by extracting desired colors using a color detection algorithm. The detected groups of pixels are called “blob”. Our shape detection algorithm extracts a simple geometric form of an object by using mathematical geometry based on probabilistic and statistical algorithms. An example of shape detection for underwater buoys is shown in Fig. 21.

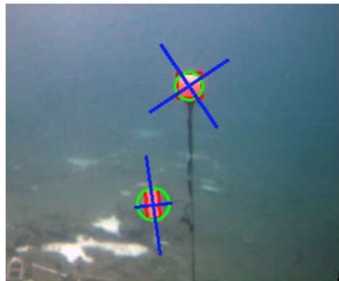


Fig. 21. Shape detection of Buoys

### E. Hydrophone processing module

Our hydrophone processing module is designed for searching an acoustic signal from the pinger. The detector is mounted under the AUV platform to measure wave heights and periods from four hydrophones as input signals.

The signals are amplified before being analyzed. Location output data are then provided. The localization configuration is shown in Fig. 22.

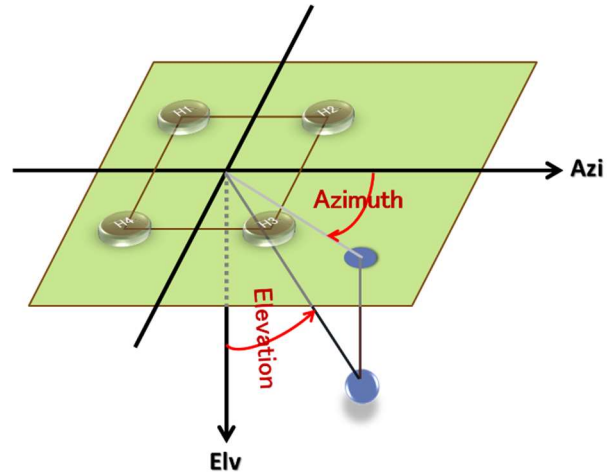


Fig. 22. Localization scenario with 4 hydrophones.

The software methodology for hydrophones carries out 4 steps.

#### 1) Sampling

This step is the beginning of DSP processing where the analog signal is converted to a digital signal.

#### 2) Pulse detection and demodulation

This step is used to detect the pinger pulses where they will be demodulated to a baseband signal.

#### 3) Delay time estimation.

Since the pulse detection algorithm may not be perfect, the delay-time estimation is used to accurately extract one pulse of pinger signals from all 4 hydrophones for further processing.

#### 4) Bearing estimation

The azimuth angle and the elevation angle are computed in this step as the output of the system. Particle filter algorithm [6] is used to reduce noises in this step. Particle filter is a general Monte Carlo (sampling) method for performing inference in state-space models where the state of a system evolves in time and information about the state is obtained via noisy measurements made at each time step. In a general discrete-time state-space model, the state of a system evolves according to

$$x_k = f_k(x_{k-1}, v_{k-1}) \tag{1}$$

where  $x_k$  is a vector representing the state of the system at time  $k$ ,  $v_{k-1}$  is the state noise vector,  $f_k$  is a possibly non-linear and time-dependent function describing the evolution of the state vector. The state vector  $x_k$  is assumed to be latent or unobservable. Information about  $x_k$  is obtained only through noisy measurements of it,  $z_k$ , which are governed by the equation:

$$z_k = h_k(x_k, n_k) \tag{2}$$

where  $h_k$  is a possibly non-linear and time-dependent function describing the measurement process and  $n_k$  is the measurement noise vector.

VI. EXPERIMENTAL RESULTS

Unfortunately, at the moment that we submitted this paper, we had not finished our vision system yet. We currently had only experimental results from our hydrophone system.

The hydrophone system experiment was setup and separated into 3 cases with different positions of the pinger. The positions are shown in Fig. 23.

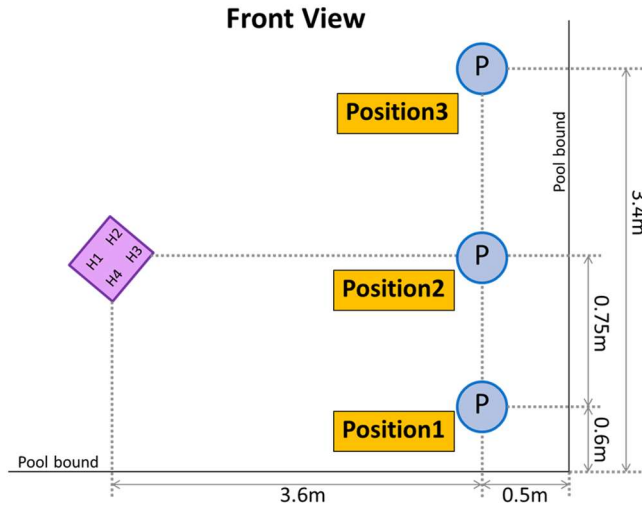


Fig. 23. Pinger location setup.

The first position is at a corner of the pool. The second position was aligned with hydrophones. The last position is far from the corner of the pool compared with the other positions.

The result of the position 1 is given in Fig. 24. The horizontal axis of this graph shows sample numbers, while the vertical axis displays amplitudes. The total time of the pulse is around 4 ms. Hence, the sampling rate of the oscilloscope is 25 kHz. The pulse was stored for about 100 samples within 4 ms. As shown in Fig. 24, the main pulse begins at around the 250th sample with the amplitude around 2 mv, and continue to around the 350th sample. After the main pulse, there are 2 echoes. One has the similar shape, but it has about 1/3 time smaller amplitude at around the 350th to the 450th samples, and another one at around the 450th to the 550th samples. After the 750th sample, we found a continuous echo until the 1300th sample.

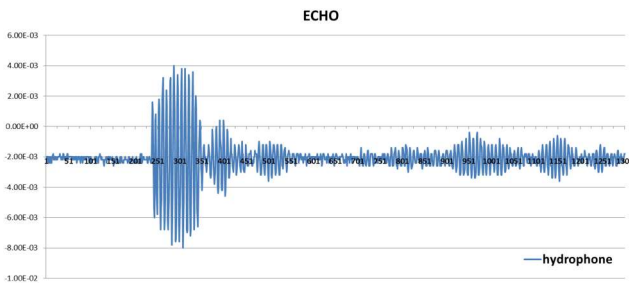


Fig. 24. Echo at position 1.

The result from the position 2 is shown in Fig. 25. The horizontal axis of this graph displays sample numbers. The

total time of the pulse is around 4 ms. Hence, the sampling rate of the oscilloscope is 25 kHz. The pulse was stored about 100 samples within 4 ms in Fig. 25. If we assume that the main pulse must arrive hydrophones first. We found that the starting point of the main pulse is at around the 200th sample with the amplitude around 4 mW, and continues to around the 300th sample. After the main pulse, there are 2 echoes. One has the similar shape, but greater amplitude at around the 300th to the 400th samples, and another one has smaller amplitude at around the 400th to the 500th sample. After the 700th sample, we found a continuous echo until the 1050th sample. As the echo cannot have greater amplitude than the main pulse, this case might happen because of the sampling rate of the oscilloscope is too low. Hence, the low amplitude data was collected at the first pulse, and the higher amplitude data were missed.

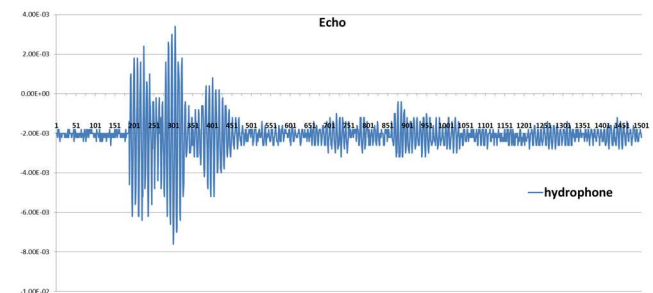


Fig. 25. Echo at position 2.

The result of the position 3 is shown in Fig. 26. The horizontal axis of this graph display sample numbers, while the vertical axis shows amplitude. The total time of the pulse is around 4 ms. Hence, the sampling rate of the oscilloscope is 25 kHz, the pulse was stored about 100 samples within 4 ms. As shown in Fig. 26, the main pulse begins at around the 120th sample with the amplitude around 2 mW, and continues to around the 220th sample. After the main pulse, there are 2 echoes. One has the similar shape but has about 1/3 time smaller amplitude at around the 220th to the 320th samples, and another one at around the 320th to the 420th samples. After the 600th sample, we found a continuous echo until the 960th sample.

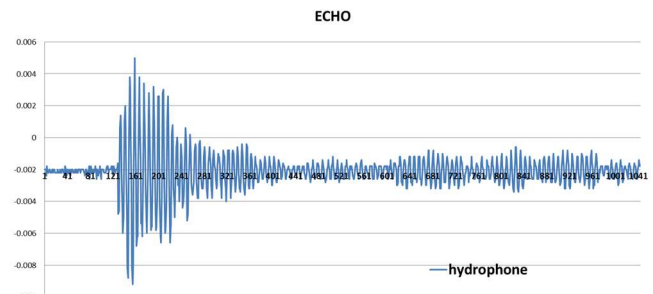


Fig. 26. Echo at position 3.

Based on these tests, we can conclude that

- 1) Our delay time estimation and bearing estimation algorithm could perform properly.
- 2) The algorithm was able to work with saturated pulses,

but the results had more errors.

3) The algorithm could compute bearing angles even if the pulse detected by a program was not the beginning of the pulse, but the results had more errors.

4) We found an unknown signal. It might be an echo or a high power noise.

5) Power detection was unstable. We have to calibrate the threshold level to cope with an unknown signal.

6) There was a pattern of 2 echoes after the main pulse in every case and small echoes after the main pulse around 24 ms.

## VII. CONCLUSION

In this team description paper, a design of Zeabus AUV was described. Technical details of designs on mechanical, electrical and software parts were covered. Unfortunately, we could not finish our vision system yet so only hydrophone system results can imply the capability of our system. Our AUV is being improved much compared to the last year. This is a good opportunity for students in the team to learn several advance algorithms and implementation with respect to their education levels. However, there are still many details that we still want to improve for better performance. We plan to implement that in Robosub 2017 too.

## ACKNOWLEDGEMENT

Zeabus AUV team has to thank many sponsors. Our highly respected main sponsors are Faculty of Engineering, Kasetsart University and PTTEP, which provides us financial supports. We appreciate staffs from Hiveground, Co. Ltd., and EmOne, Co. Ltd., for their advises to our students. Finally, we thank Kasetsart University for providing us time and space to use a university diving pool.

## REFERENCES

- [1] T. I. Fossen, "Motion control system," in *Handbook of Marine Craft Hydrodynamics and Motion Control*, 1th ed. West Sussex, UK: Wiley, 2011, ch. 12, sec. 2, pp. 365-398.
- [2] E. A. Wan and R. Van Der Merwe, "The unscented Kalman filter for nonlinear estimation," IEEE AS-SPCC, Lake Louise, AB, Canada, 2000, pp. 153-158.
- [3] A. Krizhevsky, I. Sutskever, and G. E. Hinton, "Imagenet classification with deep convolutional neural networks," *Advances in neural information processing systems*. 2012, pp. 1097-1105.
- [4] J. Canny. "A computational approach to edge detection" *IEEE Trans. PAMI*, vol. 8, no. 6, pp. 679-698, Nov. 1986.
- [5] P. Panagiotou, A. Polydoros, and P. Thiennviboon, "Multiple-Path Direction-of-Arrival Estimation for Cognitive Radio Sensing," *The 21<sup>st</sup> Annual IEEE International Symposium on Personal, Indoor, and Mobile Radio Communication*, Istanbul, 2010, pp. 791-796.
- [6] M. S. Arulampalam, S. Maskell, N. Gordon, and T. Clapp, "A tutorial on particle filters for online nonlinear/non-Gaussian Bayesian tracking," *IEEE Trans. Signal Processing*, vol. 50, no. 2, pp. 174-188, Feb. 2002.